

Neutron diffuse scattering from polar nanoregions in the relaxor $\text{Pb}(\text{Mg}_{1/3}\text{Nb}_{2/3})\text{O}_3$

K. Hirota,^{1,2,*} Z.-G. Ye,³ S. Wakimoto,^{4,1} P. M. Gehring,⁵ and G. Shirane¹

¹Department of Physics, Brookhaven National Laboratory, Upton, New York 11973-5000

²Department of Physics, Tohoku University, Sendai 980-8578, Japan

³Department of Chemistry, Simon Fraser University, Burnaby, British Columbia, Canada V5A 1S6

⁴Department of Physics, University of Toronto, Toronto, Ontario, Canada M5S 1A7

⁵NIST Center for Neutron Research, National Institute of Standards and Technology, Gaithersburg, Maryland 20899-8562

(Received 20 September 2001; published 22 February 2002)

We have studied the diffuse scattering in the relaxor $\text{Pb}(\text{Mg}_{1/3}\text{Nb}_{2/3})\text{O}_3$ (PMN) using triple-axis neutron scattering techniques. The diffuse scattering first appears around the Burns temperature $T_d \approx 620$ K, indicating that its origin lies within the polar nanoregions (PNR's). While the relative intensities of the diffuse scattering around (101), (200), and (300) are consistent with those previously reported by Vakhrushev *et al.*, they are, surprisingly, entirely different from those of the lowest-energy transverse-optic (TO) phonon. This observation led Naberezhnov *et al.* to claim that this TO mode could *not* be the ferroelectric soft mode. However, a recent neutron study by Gehring *et al.* has unambiguously shown that the lowest-energy TO mode *does* soften on cooling and that the relative intensities are similar to those of PbTiO_3 . If the diffuse scattering in PMN originates from the condensation of a soft TO mode, then the atomic displacements of the PNR *must* satisfy the center-of-mass condition. But, the atomic displacements determined from diffuse scattering intensities do not fulfill this condition. To resolve this contradiction, we propose a simple model in which the total atomic displacement consists of two components $\delta_{c.m.}$ and δ_{shift} . Here $\delta_{c.m.}$ is created by the soft-mode condensation and thus satisfies the center-of-mass condition. On the other hand, δ_{shift} represents a uniform displacement of the PNR's along their polar direction relative to the surrounding (unpolarized) cubic matrix. Within the framework of this model, we can successfully describe the neutron diffuse scattering intensities observed in PMN.

DOI: 10.1103/PhysRevB.65.104105

PACS number(s): 77.84.Dy, 61.12.-q, 77.80.Bh, 64.70.Kb

I. INTRODUCTION

Relaxors exhibit a broad maximum in the temperature dependence of the dielectric constant and a significant frequency dependence of the temperature T_{max} at which this maximum occurs. Although these peculiarities are often referred to as a “diffuse” phase transition, no macroscopic phase transition into a ferroelectric state occurs at T_{max} . Of particular interest are the lead-oxide class of relaxors. This class displays extraordinary piezoelectric properties which persist over a wide temperature range, thus presenting great appeal for device applications. Most of the lead-oxide relaxors are classified as *B*-site complex perovskite compounds, in which an average *B*-site valence of 4+ is realized by a random occupancy of two different valence cations in a fixed ratio. The prototypical lead-oxide relaxor system is $\text{Pb}^{2+}(\text{Mg}_{1/3}^{2+}\text{Nb}_{2/3}^{5+})\text{O}_3^{2-}$ (PMN) which, along with $\text{Pb}(\text{Zn}_{1/3}\text{Nb}_{2/3})\text{O}_3$ (PZN), shows an enormous increase in piezoelectric character when doped with PbTiO_3 . In spite of a decade of research, however, arguments over what intrinsic mechanism drives the diffuse transition remain unsettled.

One of the most important concepts related to the microscopic properties of relaxors is that of the so-called “polar nanoregions” (PNR's), the first experimental evidence for which was obtained by Burns and Dacol.¹ Through measurements of the optic index of refraction $n(T)$ on single-crystal specimens of several disordered ferroelectric and relaxor compounds, including both PMN and PZN, they observed that $n(T)$ deviates from a linear temperature dependence at a temperature T_d (600–650 K for PMN) far above T_{max} (≈ 265 K at 1 kHz for PMN). They proposed a model in which this

unexpected high-temperature deviation arises from small, randomly oriented, very local regions of nonreversible polarization (the PNR's) that begin to appear within the otherwise nonpolar crystal structure below T_d , which is often called the Burns temperature. Recent neutron inelastic scattering studies on PZN and PZN doped with 8% PbTiO_3 (PZN-8%PT) in their respective cubic phases at 500 K have shown that the lowest-energy transverse-optic (TO) phonon modes are overdamped for reduced wave vectors q less than a characteristic wave vector $q_{wf} \sim 0.2 \text{ \AA}^{-1}$, but underdamped otherwise.² It is now believed that this damping is caused by the PNR's because they couple strongly to the polar nature of the TO modes.

Vakhrushev *et al.*³ carried out neutron diffraction studies on PMN and observed strong diffuse scattering which remains even at 500 K. They found that the q width of the diffuse peak, which is inversely proportional to the correlation length, is temperature dependent and that both the Bragg and diffuse peaks exhibit history-dependent effects in the field-cooled (FC) and zero-field-cooled (ZFC) regimes, similar to that of a typical spin glass. The transition to this glass-like state occurs around 230 K, which is slightly below T_{max} . The diffuse scattering in PMN was subsequently measured around 16 reciprocal lattice points, from which the directions and relative magnitudes of the ionic displacements were determined.⁴ The observed diffuse scattering is broader along the direction transverse to the scattering vector \mathbf{Q} (\mathbf{Q}_\perp) than it is along the longitudinal direction (\mathbf{Q}_\parallel), a feature that is consistent with scattering from ferroelectric fluctuations. Bonneau *et al.*⁵ measured both x-ray and neutron powder diffraction from PMN and reported that addi-

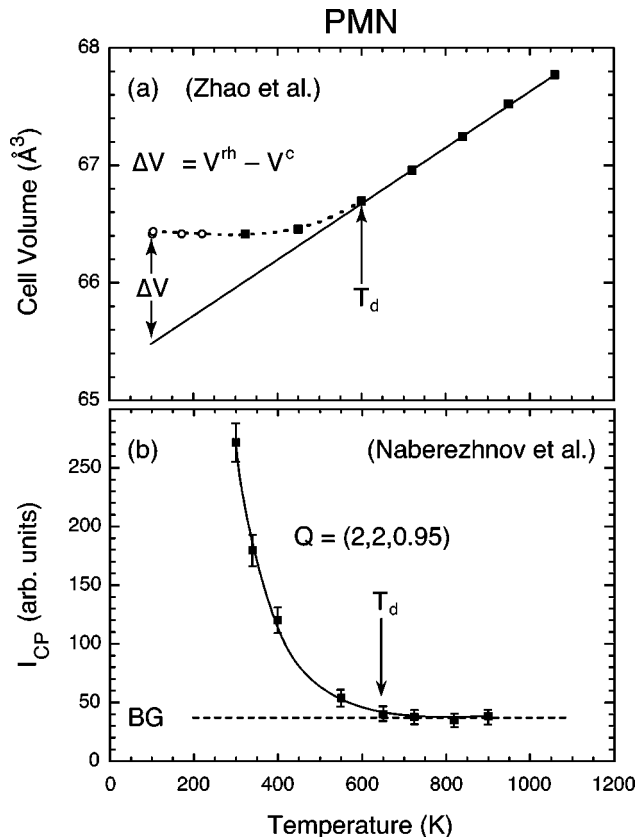


FIG. 1. (a) Temperature dependence of the unit cell volume, measured by Zhao *et al.* (Ref. 6). (b) Temperature dependence of the neutron diffuse scattering intensity (central peak) at $Q=(2,2,0.95)$, measured by Naberezhnov *et al.* (Ref. 7).

tional diffuse scattering appears in the tails of the Bragg peaks below about 600 K. Neutron powder diffraction data taken by Zhao *et al.*⁶ show a marked break in the linear temperature dependence of the cubic unit cell volume, also around 600 K, which is shown in Fig. 1(a). More recently, Naberezhnov *et al.*⁷ have confirmed that the diffuse scattering indeed becomes visible below 650 K, as shown in Fig. 1(b). These results strongly imply that the diffuse scattering in PMN results from the formation of PNR's at T_d .

Naberezhnov *et al.*⁷ have also studied the lattice dynamics of PMN using neutron inelastic scattering methods between 300 and 900 K. They calculated dynamical structure factors using the room-temperature diffuse scattering results of Vakhrušev *et al.*³ and concluded that (221) was the best zone in which to look for the ferroelectric soft mode phonon. However, they observed no underdamped soft TO phonon in the vicinity of (221) even at 900 K. Instead, they observed well-shaped peaks from the transverse-acoustic (TA) and the lowest-lying TO modes near (220), although nearly no diffuse scattering was observed around (220). They therefore concluded that the observed lowest-lying TO mode could not be identified with the ferroelectric soft mode because it exhibited a structure factor that was absolutely inconsistent with that expected from the ferroelectric diffuse scattering peak intensities. However, a recent neutron inelastic scattering study by Gehring *et al.*⁸ has unambiguously shown that

the lowest-energy zone-center TO mode does soften significantly on cooling from 1100 K to T_d , below which it becomes overdamped, and that the relative phonon intensities measured in different zones are very similar to those found in PbTiO_3 , a prototypical (displacive) ferroelectric system.

It is thus clear that an important discrepancy exists between the relative intensities of the soft TO mode and those of the diffuse scattering in PMN. Since each is related to either dynamic or static atomic displacements toward the same ferroelectric state, the relative intensities should be consistent. The aim of this paper is to determine how the diffuse scattering in PMN connects to the soft TO mode and thereby resolve this discrepancy. To study the diffuse scattering in PMN in detail, we have carried out neutron diffraction measurements from 200 to 700 K. We have concentrated on the diffuse scattering around the three Bragg reflections (101), (200), and (300) and measured the q profiles and temperature dependence. These results, as well as the experimental conditions, are summarized in Sec. II. In Sec. III we describe our phonon structure factor calculations using the atomic displacements determined from the diffuse scattering intensities, which helps to clarify the inconsistency between the relative intensities of the soft TO mode and of the diffuse scattering. We believe this discrepancy can only be resolved if one assumes the simple model in which the PNR's are shifted along their polar direction relative to the surrounding cubic matrix. Finally, we compare our experimental results with those from previous neutron and x-ray scattering studies and discuss one possible origin of this concept, which we call a "phase-shifted condensed soft mode," in Sec. IV.

II. DIFFUSE SCATTERING

The neutron diffuse scattering data presented here were obtained on the BT9 triple-axis spectrometer located at the NIST Center for Neutron Research. The data were taken with fixed incident neutron energy $E_i=14.7$ meV ($\lambda=2.36$ Å) and with horizontal beam collimations $40'-46'-S-40'-80'$ or $40'-10'-S-10'-80'$ ("S"=sample). Single crystals of PMN were grown by a top-seeded solution growth technique using PbO as flux. The growth conditions were determined based on the pseudobinary phase diagram established from PMN and PbO .⁹ An as-grown single crystal with a nearly half-cubic morphology, having a volume of 0.4 cm³ and a weight of 3.25 g, was used for the diffuse scattering measurements. The crystal exhibits three naturally grown $\{100\}_{cubic}$ facets and was mounted on a boron nitride post using tantalum wire with one of the facets facing vertically and then attached to the cold-head of a high-temperature closed-cycle helium refrigerator. This orientation gave access to reflections of the form $(h0l)$ in the scattering plane. The lattice constant of PMN is $a=4.04$ Å at room temperature; thus, 1 rlu (reciprocal lattice unit) corresponds to $2\pi/a=1.553$ Å⁻¹.

Figure 2(a) shows peak profiles of the transverse diffuse scattering in the vicinity of (101). Note that the y axis is displayed on a logarithmic scale. At 690 K, there is no diffuse scattering. The peak profile is well described by a Gaussian function with a full width at half maximum (FWHM) corresponding to that of the instrumental q resolu-

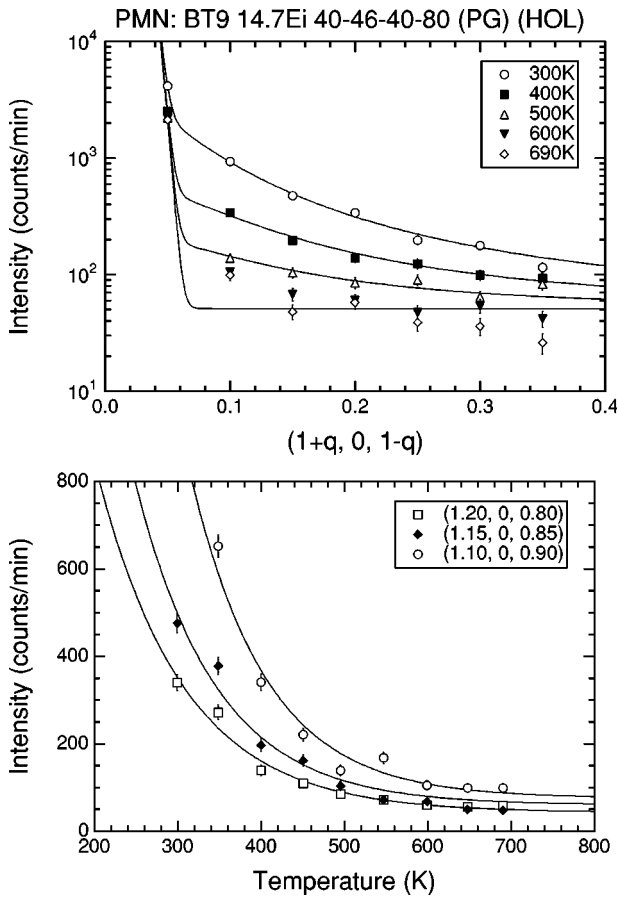


FIG. 2. (a) Diffuse scattering profiles around (101) along $[10\bar{1}]$ at 300, 400, 500, 600, and 690 K. Curves are fits to a combination of Gaussian (Bragg peak) and Lorentzian (diffuse scattering) line shapes. (b) Temperature dependence of the diffuse scattering intensities at (1.20,0,0.80), (1.15,0,0.85), and (1.10, 0,0.90). The diffuse scattering clearly begins increasing around T_d .

tion at the (101) Bragg peak. With decreasing temperature, a weak signal starts to emerge out of the (101) Bragg peak, growing more rapidly as the temperature is lowered. The observed diffuse scattering can be nicely fit with a Lorentzian function as shown in Fig. 2(a). The temperature dependence of the diffuse scattering is more clearly presented in Fig. 2(b). The diffuse scattering appears below about 600–650 K, consistent with the Burns temperature $T_d \sim 620$ K for PMN, and increases almost exponentially with decreasing temperature.

The diffuse scattering peak profiles were more closely examined by employing a tighter collimation of $40'-10'-S-10'-80'$. Figure 3 depicts the transverse diffuse scattering profiles at (101), (200), and (300) at 300 and 370 K. Although the difference in the diffuse scattering intensity between these two temperatures is not very large, as is apparent from Fig. 2, it is nevertheless discernable at (101). A significantly larger difference is observed at (300), which indicates that the diffuse scattering is stronger at (300) than at (101). No difference in intensity at finite q near (200) was found, which suggests the diffuse scattering is very weak at (200). We speculate that the tail-like feature near $q=0$ for

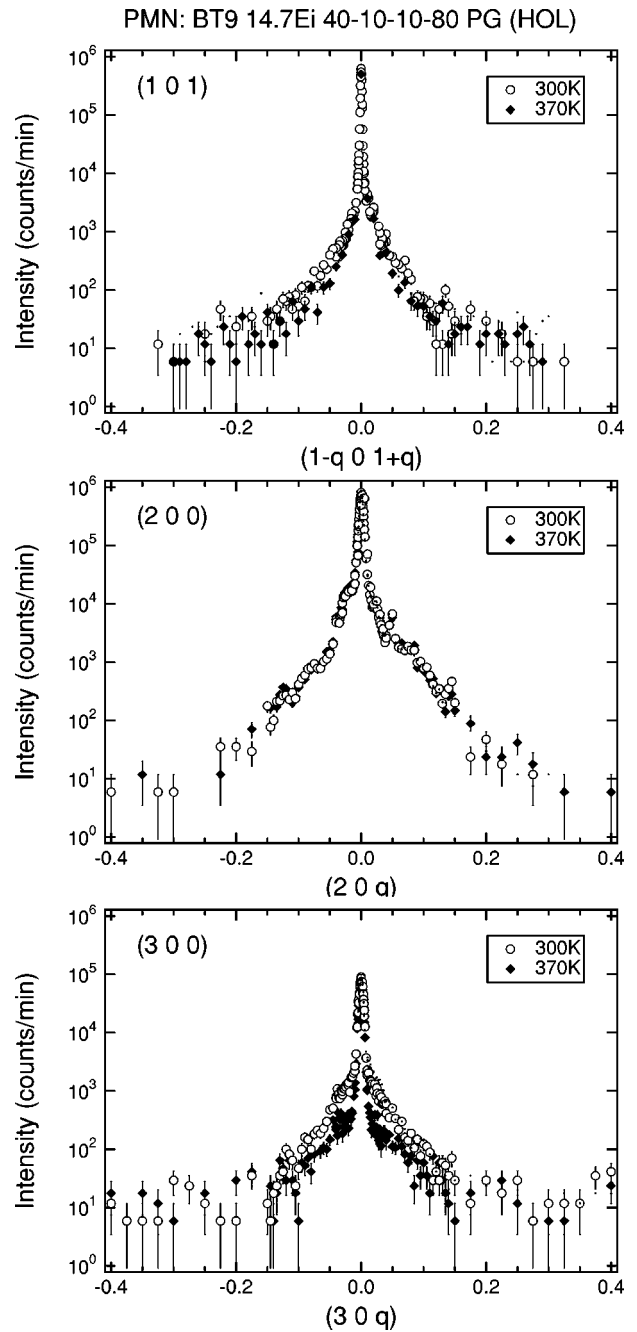


FIG. 3. Profiles of the diffuse scattering peaks at (a) $(1-q, 0, 1+q)$, (b) $(2, 0, q)$, and (c) $(3, 0, q)$ at $T=300$ and 370 K.

(200) is due to contamination from the TA phonon, which is quite strong near (200), as some TA-mode scattering will inevitably spill into the elastic profile because of the imperfect instrumental energy resolution. The relative intensities of the (101), (200), and (300) diffuse scattering peaks are consistent with those reported in the previous neutron diffraction measurement by Vakhruhev *et al.*³ We have also carried out a detailed survey of the (101) diffuse scattering, the results of which are shown in Fig. 4. The diffuse scattering is highly elongated along the direction transverse to the scattering vector, which is also consistent with the previous report.³ Similar neutron diffuse scattering results at (101) and

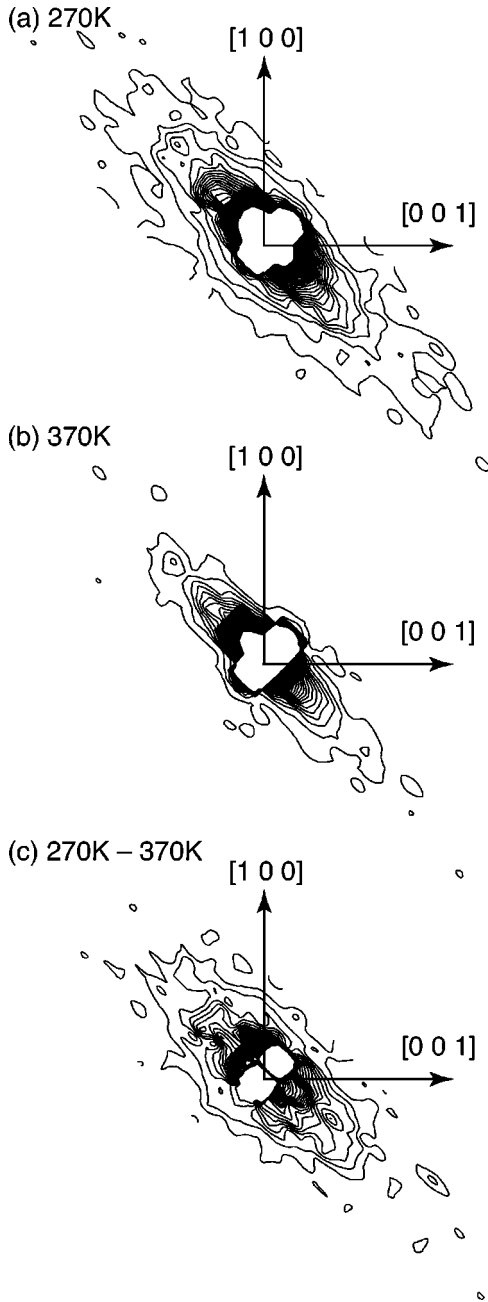


FIG. 4. Intensity contours of the diffuse scattering around (101) at (a) 270 K and (b) 370 K. (c) Difference between (a) and (b).

(200) were recently observed by Koo *et al.* in a single-crystal sample of PMN doped with 20% PbTiO_3 .¹⁰

III. FERROELECTRIC PHONON

Gehring *et al.*⁸ have recently reported that the lowest-energy zone-center TO mode in PMN softens on cooling from 1100 K to T_d and that the relative intensities measured in different zones are very similar to those found in PbTiO_3 . This result sharply contradicts the fact that the relative intensities of the diffuse scattering in different zones are entirely different from those of the lowest-energy TO phonons, an observation which led Naberezhnov *et al.*⁷ to claim that the

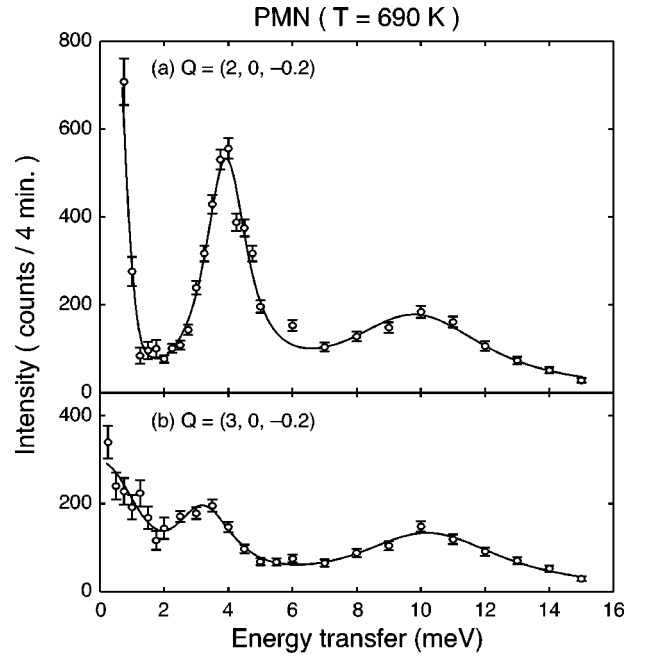


FIG. 5. Energy spectra of the transverse acoustic and optic phonons at 690 K, i.e., above the Burns temperature T_d , around (a) (200) and (b) (300).

lowest-energy TO mode could *not* be the ferroelectric soft mode. To understand how PMN undergoes the *diffuse transition* through the formation of the PNR, this contradiction must be resolved. In this section, we reexamine the soft mode of PMN and introduce a new concept, the “phase-shifted condensed soft mode,” as a microscopic description of PNR formation.

As shown in the previous section, we observe no diffuse scattering around (200), consistent with previous reports. However, TO phonons are clearly observed around both (200) and (300) as shown in Fig. 5, which shows two constant- Q scans at 690 K (i.e., above the Burns temperature T_d) at $(2,0,-0.2)$ and $(3,0,-0.2)$. The solid curves are fits to two Lorentzian functions of E , the neutron energy transfer, convolved with the proper instrumental resolution function. From the fitting results, the ratio of the two TO phonon intensities is

$$\frac{|F_{obs}(200)|^2}{|F_{obs}(300)|^2} = 1.24 \pm 0.20. \quad (1)$$

According to the pioneering work by Harada *et al.*,¹¹ which describes the determination of the normal-mode vibrational displacements in perovskites from measured phonon intensities, the relative intensities of phonons are determined mostly by the ratio of two dominant modes, i.e., the Slater mode and the Last mode. In the Slater mode, the oxygen and Mg/Nb (MN) atoms vibrate in opposition while the Pb atoms remain stationary. The Last mode corresponds to opposing motions of the $(\text{Mg/Nb})\text{O}_6$ octahedra and the Pb atoms. In both modes, the three oxygen atoms in the unit cell move as a rigid unit. We define the ratio of the two modes as S

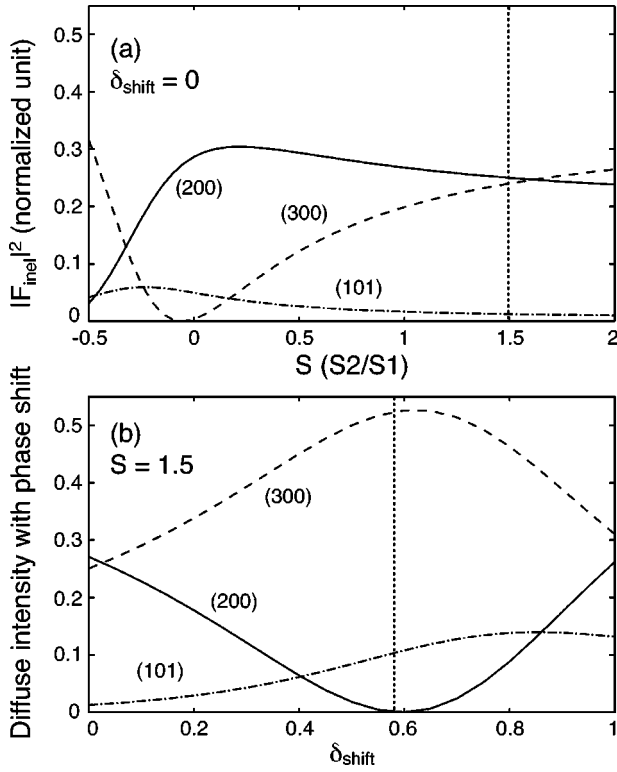


FIG. 6. (a) Calculated intensities of the TO phonon mode at (101), (200), and (300) as a function of the ratio S between the S_1 (Slater) and S_2 (Last) modes. (b) Calculated intensities of the TO phonon mode at (101), (200), and (300) as a function of the phase shift of the PNR along their polar direction relative to the surrounding cubic matrix.

$= S_2/S_1$, where S_1 and S_2 represent the contribution from the Slater mode (s_1) and Last mode (s_2), respectively.

Let us first determine the ratio S . Figure 6(a) shows the inelastic structure factors $|F_{inel}|^2$ at (101), (200), and (300) as a function of S , which are calculated using the formula given by Harada *et al.*¹¹ In this calculation, we assume that the atomic displacements \mathbf{s}_1 and \mathbf{s}_2 are parallel to the [100] direction for the sake of simplicity. Combining Eqs. (1) and (5) of Ref. 11, we have obtained $|F_{inel}|^2$ for the lowest branch at the zone center ($\mathbf{q}=0$) using constant- \mathbf{Q} scans as follows:

$$|F_{inel}|^2 = \sum_{\kappa} [\mathbf{Q} \cdot \xi_{\kappa}] b_{\kappa} \exp(-W_{\kappa}) \exp(i\mathbf{G} \cdot \mathbf{R}_{\kappa}), \quad (2)$$

where the scattering vector (\mathbf{Q}) is the sum of the reciprocal lattice vector (\mathbf{G}) and the phonon wave number ($\mathbf{q}=0$), and the normalized displacement vector for the κ th atom, ξ_{κ} , in our condition is

$$\xi_{\kappa} = \mathbf{s}_{\kappa 1} + S \mathbf{s}_{\kappa 2}. \quad (3)$$

From Table 1 of Ref. 11, the atomic displacements along the [100] direction are

$$\xi_{\text{Pb}} = -Sk',$$

$$\xi_{\text{MN}} = -k + S,$$

$$\xi_{\text{O}} = 1 + S, \quad (4)$$

where the center-of-mass condition requires $k = 3M(\text{O})/M(\text{MN}) = 0.686$ and $k' = [M(\text{MN}) + 3M(\text{O})]/M(\text{Pb}) = 0.596$. The calculated values are normalized by the sum of $|F_{inel}|^2$ over all reflections that can be reached with an incident neutron energy $E_i = 14.7$ meV: (100), (110), (200), (210), (220), (300), (310), and their equivalent. Debye-Waller factors $\exp(-W_{\kappa}) = \exp(-B_{\kappa}|\mathbf{Q}/4\pi|^2)$ are calculated using $B_{\text{Pb}} = 0.915$ and $B_{\text{NM}} = 0.483$ and $B_{\text{O}} = 1.02$.¹² Figure 6(a) indicates that the experimentally observed intensity ratio of $|F_{obs}(200)|^2/|F_{obs}(300)|^2 = 1.24$ obtained in Eq. (1) is realized between $S = 1.0$ and 1.5 .

If the diffuse scattering of PMN originates from the condensation of the soft TO mode, then the above formula should be also applicable to the diffuse scattering intensities and that the atomic displacements determined from the diffuse scattering intensities must also satisfy the center-of-mass condition

$$\sum_{\kappa} \delta(\kappa) M(\kappa) = 0, \quad (5)$$

where $\delta(\kappa)$ and $M(\kappa)$ are the displacement and the atomic mass of the κ th atom, respectively. However, the values $\delta(\kappa)$ determined from the diffuse scattering intensities by Vakhrushev *et al.*,⁴

$$\delta(\text{Pb}) = 1.00, \quad M(\text{Pb}) = 207,$$

$$\delta(\text{MN}) = 0.18, \quad M(\text{MN}) = 70,$$

$$\delta(\text{O}) = -0.64, \quad M(\text{O}) = 16, \quad (6)$$

do *not* satisfy the center-of-mass condition. This contradiction is a natural corollary to the observed inconsistency between the relative intensities of the diffuse and the soft TO mode scattering.

To resolve this discrepancy, we propose a simple model in which the atomic displacements consist of two components, $\delta(\kappa) = \delta_{c.m.}(\kappa) + \delta_{shift}$. In this model, $\delta_{c.m.}$ is induced by the condensation of the soft mode, and thus satisfies the center-of-mass condition. On the other hand, δ_{shift} shifts the PNR along their polar directions relative to the surrounding cubic matrix, which is, in other words, a phase shift. By applying this model, the $\delta(\kappa)$ values listed in Eq. (6) can be separated into two parts:

$$\delta_{c.m.}(\text{Pb}) = 0.42,$$

$$\delta_{c.m.}(\text{MN}) = -0.40,$$

$$\delta_{c.m.}(\text{O}) = -1.22, \quad (7)$$

and

$$\delta_{shift} = 0.58. \quad (8)$$

Note that the $\delta_{c.m.}$ values are uniquely determined from the center-of-mass condition and can be further decomposed into contributions from the Slater mode and the Last mode. The

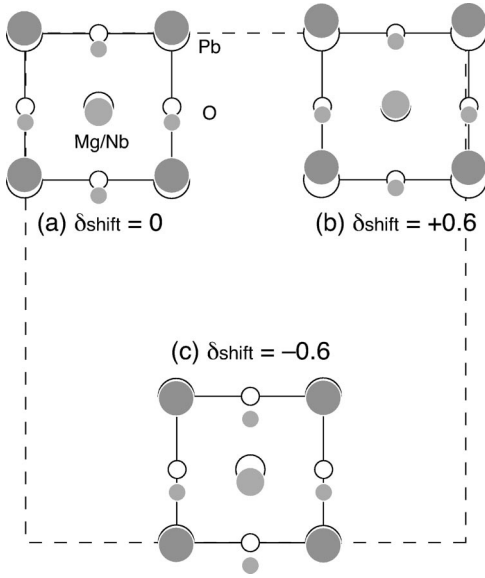


FIG. 7. Atomic displacements corresponding to three different phase shift values: (a) $\delta_{shift}=0$, (b) $\delta_{shift}=0.6$, and (c) $\delta_{shift}=-0.6$. The open circles represent the normal atomic positions without displacement, whereas the shaded circles show the atomic positions with both displacement and shift.

corresponding ratio S between the Slater mode and Last mode contributions is 1.5, which is consistent with the value obtained in Fig. 6(a). Note that the phase shift δ_{shift} becomes effective only when the PNR condense out from the soft TO mode. Hence the phonon intensities are determined only by the $\delta_{c.m.}$ values.

Now that we have confirmed that the $\delta_{c.m.}$ values derived from the diffuse scattering intensities are consistent with the inelastic scattering intensities of the soft TO mode, we can calculate how the diffuse scattering intensities depend on the phase factor δ_{shift} with the constraint $S=1.5$ using the $\delta_{c.m.}$ values listed in Eq. (7). The results are shown in Fig. 6(b). Note that the values at $\delta_{shift}=0$ are identical to those at $S=1.5$ in Fig. 6(a) as expected. At $\delta_{shift}=0.58$, which was derived above to satisfy the center-of-mass condition, the diffuse intensity around (200) approaches zero, in agreement with experiment. Thus, our “phase-shifted condensed soft-mode” model consistently explains both the diffuse scattering and the soft-mode intensities from the same atomic displacements.

Last, we consider the phase shift from the crystal lattice point of view. Figure 7 depicts the atomic displacements schematically with three different phase shift values. Figure 7(a) shows the displacements of Eq. (7) without the phase shift, which satisfies the center-of-mass condition and gives the same relative intensities for both the diffuse scattering and the soft TO mode. However, once all the atoms undergo an additional shift along the same direction by the same amount $\delta_{shift}=+0.6$, the center-of-mass condition is no longer satisfied, resulting in the *accidental* disappearance of the (200) diffuse neutron scattering intensity. Figure 7(c), which depicts a uniform shift of $\delta_{shift}=-0.6$, is shown just for comparison.

IV. DISCUSSION

In the preceding sections we have demonstrated how the inconsistency between the diffuse scattering and the soft-TO-mode intensities is explained naturally within the framework of a “phase-shifted condensed soft mode.” Our data on the diffuse scattering cross sections in three different Brillouin zones along with our measurements of the soft-TO-mode phonons in two different zones serve as a confirmation of the detailed measurements already published by other groups.^{3–5,7} But while our data are in agreement, our interpretations differ entirely. The simplicity of our model argues in its favor. Other than the standard picture of condensed local ferroelectric fluctuations created by a soft phonon, there is only one added feature, that being a uniform phase shift of the PNR’s relative to the surrounding cubic matrix. We believe the simpler solution is the correct one.

The process of separating the observed atomic displacements into optic-mode displacements $\delta_{c.m.}$ and a single-phase-shift parameter δ_{shift} is straightforward and unique, and requires no adjustable parameters. We realized this fact a long time ago. We did not recognize, however, the significance of the derived center-of-mass structure. Only recently, when the true soft mode of PMN was observed directly by neutron scattering at high temperature,⁸ did we recognize the identity of the diffuse structure as a condensed soft mode. Then the idea of the phase shift followed naturally. But one important question still remains: *what is the microscopic origin of this phase shift?* It should be emphasized that the direction of the phase shift is not arbitrary as is clear from Fig. 7. Our model requires that the phase shift be parallel, not antiparallel, to the polarization resulting from the atomic displacement. Under zero external electric field, as is the case here, the polarization direction of a single PNR can be parallel to any symmetric direction of $\langle 111 \rangle$, i.e., $[111], [\bar{1}\bar{1}\bar{1}], \dots, [1\bar{1}\bar{1}]$.¹³ Therefore, the phase-shifted directions of the PNR’s are microscopically aligned to their polarizations, although they appear macroscopically random. Then, *why is the phase shift of the PNR parallel to their polarization?*

We speculate that microscopic inhomogeneities in the site occupancy of the Mg^{2+} and Nb^{5+} cations produce a local electric field gradient that determines the direction of polarization of the PNR. In other words, a nanoregion exposed to a local field gradient becomes a *polar* nanoregion with a polarization parallel to the gradient. Once a PNR is formed, its polarization starts to interact with the local field gradient and may result in shifting the PNR in order to compensate for the Coulomb interaction with the lattice distortion due to the phase shift. The phase shift in this case is parallel to the local field gradient and thus to the polarization of the PNR. Since the microscopic inhomogeneities associated with the spatial distribution of the Mg^{2+} and Nb^{5+} cations causes random charged domains, the local field gradient is random. Therefore, the polarizations of the PNR should also be random. However, as explained above, the phase shift of a particular PNR is always parallel to its polarization. These descriptions are still qualitative and need to be tested experimentally. It is particularly important to study the mi-

croscopic properties of the PNR, such as their correlation lengths and textures as a function of temperature as well as electric field. We also need to understand the chemical inhomogeneity of Mg^{2+} and Nb^{5+} microscopically.

Finally, our model should help to resolve some of the conflicting x-ray diffuse scattering interpretations.^{14–16} The diffuse intensity around (200) is only accidentally zero when measured with neutrons, but it should be nonzero when measured with x rays because of the differences between the neutron nuclear scattering lengths and the x-ray atomic scattering factors.

In summary, we have studied the diffuse scattering of the relaxor $\text{Pb}(\text{Mg}_{1/3}\text{Nb}_{2/3})\text{O}_3$ over a wide temperature range with neutron scattering techniques. We have confirmed that the relative intensities are consistent with previous reports and that the diffuse intensity starts increasing below the Burns temperature T_d . We have revisited the soft transverse-optic mode, the existence of which has been recently confirmed, and examined the inconsistency between the soft phonon and diffuse intensities. We have proposed a concept, the “phase-shifted condensed soft mode,” which naturally explains the inconsistency as well as the microscopic origin of the formation of the polar nanoregions.

ACKNOWLEDGMENTS

We would like to thank W. Chen for his valuable help in the growth of the PMN crystal, Y. Fujii, D. Neumann, B. Noheda, K. Ohwada, H. You, and S. Vakhrushev for stimulating discussions, and especially N. Takesue for sharing with us his recent x-ray scattering results on PMN. This work was supported mainly by the U.S. - Japan Cooperative Research Program on Neutron Scattering between the U.S. Department of Energy and the Japanese MONBU-KAGAKUSHO and in part by a Grant-In-Aid for Scientific Research from the MONBU-KAGAKUSHO. We also acknowledge financial support from the U.S. DOE under Contract No. DE-AC02-98CH10886 and the Office of Naval Research under Grant No. N00014-99-1-0738. Work at the University of Toronto is part of the Canadian Institute for Advanced Research and is supported by the Natural Science and Engineering Research Council of Canada. We acknowledge the support of the NIST Center for Neutron Research, the U.S. Department of Commerce, for providing the neutron facilities used in the present work.

*Corresponding author: hirota@iiyo.phys.tohoku.ac.jp

¹G. Burns and F.H. Dacol, *Solid State Commun.* **48**, 853 (1983).

²P.M. Gehring, S.-E. Park, and G. Shirane, *Phys. Rev. Lett.* **84**, 5216 (2000); *Phys. Rev. B* **63**, 224109 (2001).

³S.B. Vakhrushev, B.E. Kvyatkovksy, A.A. Naberezhnov, N.M. Okuneva, and B. Toperverg, *Ferroelectrics* **90**, 173 (1989).

⁴S.B. Vakhrushev, A.A. Naberezhnov, N.M. Okuneva, and B.N. Savenko, *Phys. Solid State* **37**, 1993 (1995).

⁵P. Bonneau, P. Garnier, G. Calvarin, E. Husson, J.R. Gavarrri, A.W. Hewat, and A. Morell, *J. Solid State Chem.* **91**, 350 (1991).

⁶J. Zhao, A.E. Glazounov, Q.M. Zhang, and B. Toby, *Appl. Phys. Lett.* **72**, 1048 (1998).

⁷A. Naberezhnov, S. Vakhrushev, B. Dorner, D. Strauch, and H. Moudden, *Eur. Phys. J. B* **11**, 13 (1999).

⁸P.M. Gehring, S. Wakimoto, Z.-G. Ye, and G. Shirane, *Phys. Rev. Lett.* **87**, 277601 (2001).

⁹Z.-G. Ye, P. Tissot, and H. Schmid, *Mater. Res. Bull.* **25**, 739 (1990).

¹⁰T.Y. Koo, P.M. Gehring, G. Shirane, V. Kiryukhin, S.-W. Cheong, and S.G. Lee, cond-mat/0110531 (unpublished).

¹¹J. Harada, J.D. Axe, and G. Shirane, *Acta Crystallogr., Sect. A: Cryst. Phys., Diffr., Theor. Gen. Crystallogr.* **26**, 608 (1970).

¹²A. Verbaere, Y. Piffard, Z.-G. Ye, and E. Husson, *Mater. Res. Bull.* **27**, 1227 (1992).

¹³Note that the polarization along $\langle 111 \rangle$ is a superposition of three $\langle 100 \rangle$ components. We have chosen only one of them and have described our model along that direction. However the more general case of $\langle 111 \rangle$ is easily derived from this.

¹⁴S. Vakhrushev, A. Naberezhnov, S.K. Sinha, Y.P. Feng, and T. Egami, *J. Phys. Chem. Solids* **57**, 1517 (1996).

¹⁵H. You and Q.M. Zhang, *Phys. Rev. Lett.* **79**, 3950 (1997).

¹⁶N. Takesue, Y. Fujii, and H. You, *Phys. Rev. B* **64**, 184112 (2001).